Deuterium NMR Study of the Dynamics of Self-Assembled Hexadecanoate Monolayers on Zirconium Oxide

C. T. Yim*

Department of Chemistry, Dawson College, 3040 Sherbrooke Street West, Westmount, Québec, Canada H3Z 1A4

A. O'Donnell, K. Yach, F. G. Morin, and L. Reven

Department of Chemistry, McGill University, 801 Sherbrooke Street West, Montréal, Québec, Canada H3A 2K6

Received: March 25, 2003; In Final Form: October 6, 2003

Deuterium NMR spectroscopy has been used to probe the dynamics of two samples, 2,2-d_2-hexadecanoate (HDCA) and perdeuterated HDCA monolayers on nonporous ZrO_2 powder (surface area $\sim$ 40 m^2/g) over the temperature range of 180 K to room temperature. The data indicate the presence of a considerable motional gradient in the tethered chain. Line shape simulations were performed on the spectra of 2,2-d_2-HDCA to extract detailed information on the dynamic processes involved. These quantitative line shape analyses clearly show that, over the whole temperature range studied, the C2—D bonds have substantial motional freedom with respect to the characteristic ^{2}H NMR time scale. In addition, at each temperature, a weighted superposition of several simulated line shapes with different rates and site populations is required to account for the observed spectral features, indicating the presence of considerable motional heterogeneity within the hexadecanoate monolayers. The results will be compared with dynamic behaviors of other self-assembled monolayers (SAMs), particularly those of alkylthiolate SAMs on gold nanoparticles and phosphonate SAMs on ZrO_2 powder. Attempts will be made to delineate the effects of various factors on the alkyl chain dynamics.

Introduction

Self-assembled monolayers (SAMs) and multilayers of long-chain molecules are of interest for both their fundamental importance in understanding interfacial interactions and their potential applications in material science. Among the first SAMs to be studied were monolayers of alkanoic acids on metal oxides probably because of their close resemblance to the widely studied Langmuir−Blodgett films of alkanoic acids.[1−3] Monolayers and multilayers formed by other organic acids particularly those of phosphonic acids have also enticed the increasing attention of many investigators.[4−8] During the past few years, a vast array of experimental techniques has been used for characterizing the structures of these SAMs, yielding a picture of densely packed oriented monolayer assemblies with fine differences in structural details and in properties depending on the binding amphiphiles as well as the substrates.[2,9,10] For example, it was revealed that alkanoic acids bind to AgO and ZrO_2 through a bidentate surface bond and more weakly to aluminum or copper oxide via a monodentate attachment.[1c,11,12] A solid-state NMR study by this group demonstrates that alkanoate monolayers on zirconium oxide display chain conformation, mobility, and reversible order/disorder transitions similar to other SAMs.[12] However, most studies concerning the monolayers of organic acids on metal oxides deal with static or time-averaged properties such as binding geometries and orientational and conformational orders, and direct experimental investigations of dynamic properties are relatively rare. Recently, an electron spin resonance (ESR) study of chain dynamics of self-assembled stearic acid films grown on an Al_2O_3 film was reported. It reveals a distinct dependence of the onset of the rotational motion on the location of the spin-label along the chain.[13]

Various solid NMR techniques have been employed to examine the microstructure and dynamics of SAMs.[10b] Among the commonly accessible nuclei, the deuteron has been a powerful probe for studying molecular dynamics in solid and in other anisotropic systems. It is well established that deuterium NMR is dominated by quadrupolar interactions and is almost exclusively governed by the motions and orientation of the deuteron-containing bond (e.g., the C−D bond) relative to the applied magnetic field. Dipolar interactions with other magnetic nuclei present in the system, most importantly protons, show a negligible effect on the observed spectra. Various motional models have been proposed for evaluating the type, the amplitudes, and the rates of motions that affect the observed ^{2}H line shapes and relaxation times.[14−16] Studies of this nature have provided valuable information on the dynamics of surface groups of modified silica in the "dry" state and in the presence of wetting solvents.[17,18] Lately, we have also reported the results of a detailed deuterium NMR study of 1,1-d_2-octadecylphosphonate (ODPA-d_2) SAMs on zirconium oxide powder.[19] It was demonstrated that, over the whole temperature range studied, the C1—D bonds of ODPA molecules have substantial motional freedom on the characteristic ^{2}H NMR time scale. In addition, considerable motional heterogeneity is present within the ODPA monolayers. These and other experiments also show that the low S/N ratios observed for the samples restrict the method to systems with large surface area.

* To whom correspondence should be addressed. Phone: (514) 931-8731. Fax: (514) 931-3567. E-mail: c.yim@mcgill.ca.

10.1021/jp0347623 CCC: $27.50
Published on Web 12/31/2003

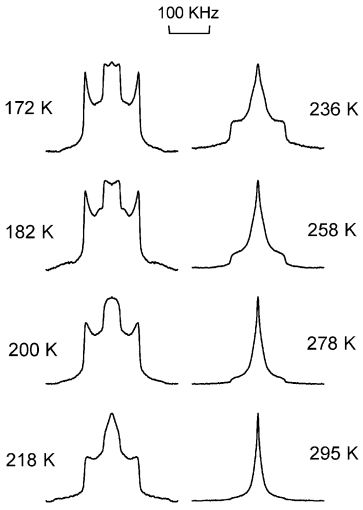

Figure 1. ^{2}H NMR spectra of HDCA-d_{31} adsorbed on ZrO_2 at various temperatures, recorded with pulse spacing $\tau = 40$ μs.

In this paper, we report the measurements of ^{2}H NMR spectra of hexadecanoate molecules, perdeuterated (HDCA-d_{31}) and specifically deuterated at position 2 (HDCA-d_2), adsorbed on nonporous ZrO_2 powder. The spectra were acquired as functions of temperature and of echo delay time τ. The site-specific deuteration at position 2 allows us to focus our attention on the headgroup-substrate interactions and examine their effect on the chain dynamics.

Experimental Section

Nonporous zirconia, ZrO_2, powder with a reported surface area of 40 m^2/g and an average particle size of 30 nm was obtained from Degussa Corp. The powder was calcinated at 400 °C overnight to eliminate any residue organic impurities. Perdeuterated and 2,2-d_2-hexadecanoic acids were obtained from Cambridge Isotope Lab, Inc., and used without further purification. Monolayer samples were prepared as described before,[12] except that 2−3 times excess, instead of 5 times excess, needed to form a complete monolayer was used in the preparations.

Elemental analyses show that the carbon contents of the monolayer samples are 2.97% for HDCA-d_{31} and 2.52% for HDCA-d_2. Assuming a surface area of 40 m^2/g for the ZrO_2 powder and 30×10^{-10} m^2 area/HDCA molecule, the corresponding surface coverage for the two samples was estimated to be 73% and 61%, respectively.

The ^{2}H NMR spectra were acquired with a Chemagnetics CMX-300 spectrometer operating at 45.99 MHz using the phase alternating quadrupolar echo sequence. The acquisition conditions and parameters were as follows: number of acquisitions, 7000−25 000; $\pi/2$ pulse length, 2.0−4.0 μs; acquisition recycle time, 1.0 s; dwell time, 1.0 μs; pulse delay time τ, 20−80 μs. After Fourier transformation, the resulting spectra were further symmetrized by reversing the recorded pattern through the center and adding to itself. The signal intensity was measured from the height of the echo maximum.

Simulations of deuterium powder line shapes were performed with a modified Wittebort program.[20,21] All calculated line shapes were corrected for finite pulse length and convoluted with a Lorentzian broadening of 1.5 kHz.

Results

The deuterium spectra of the fully deuterated hexadecanoate monolayers, recorded with $\tau = 40$ μs are shown in Figure 1 as a function of temperature. At the lowest temperature (172 K), the observed spectrum consists of a motionally narrowed Pake doublet superimposed on top of another doublet having rigid-lattice width of ∼120 kHz; they can be respectively attributed to the methyl and methylene groups in the alkyl chain. The terminal CD_3 group is expected to execute rapid rotation about its 3-fold symmetry axis yielding a powdered pattern with a splitting of ∼42 kHz. The narrow doublet observed at 172 K shows a doublet splitting of only ∼35 kHz, suggesting the presence of restricted wobbling of the 3-fold axis probably due to the libration motions of the upstream methylene groups. With increasing temperature, the central doublet gradually changes to a triangular peak and its relative intensity increases at the expense of the broader signal of 120 kHz breadth. At room temperature the broader component is reduced to a barely noticeable base under a relatively narrow and featureless peak.

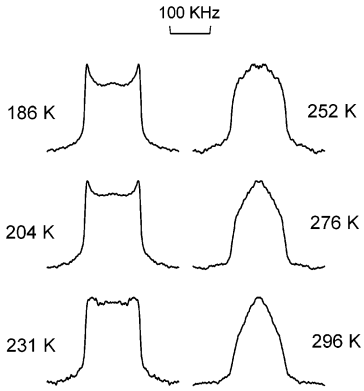

Figure 2. ^{2}H NMR spectra of HDCA-2,2-d_2 adsorbed on ZrO_2 at various temperatures, recorded with pulse spacing $\tau = 20$ μs.

Because the broader signal is composed of contributions from less mobile methylene groups in the fully deuterated sample, the variation of spectral features with temperature mainly reflects the increased molecular mobility toward the untethered chain end. Starting from the untethered end, the raising temperature renders successive methylene groups sufficiently mobile so that the powder spectrum arising from these individual methylene groups becomes a relatively narrow and featureless peak. They contribute to the observed intensity of the narrow central peak rather than the broad signal, causing corresponding changes in the relative intensities of the narrow and broad signals. At room temperature, the motions of methylene groups adjacent to the headgroup remain restricted and their spectrum exhibits a breadth of ∼120 kHz. These spectral features can be easily noticed in the spectra of HDCA-d_{31} and HDCA-d_2 samples shown in Figures 1 and 2 (see discussion below), respectively. These rationales lead us to conclude that, in our monolayer system, there exists a significant motional gradient along the alkyl chain. The motional gradient along the tethered alkyl chain has also been observed in other systems.[13,17,22,23]

Figure 2 shows the quadrupole echo spectra of the HDCA-d_2 monolayer sample, recorded with $\tau = 20$ μs, as a function of temperature. At 200 K, the observed spectrum is a Pake doublet with distinct nonrigid characteristics, mainly the broader horns and a raised middle hump. These nonrigid features testify that, even at this low temperature, the C2−D bonds are sufficiently mobile to affect the observed spectrum. With increasing temperature, the relative intensity of the central portion of the spectrum gradually increases with respect to that of the two horns and a relatively broad spectrum with a triangular top is observed at room temperature. However, the breadth of the powder spectra remains more or less unchanged at approximately 120 kHz.

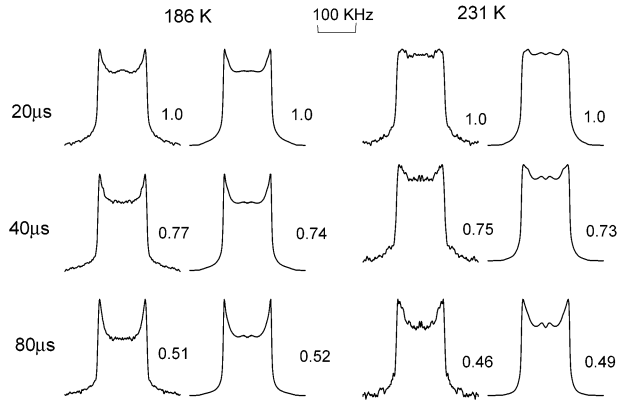

Figure 3. Experimental (left) and simulated (right) ^{2}H NMR spectra of HDCA-2,2-d_2 on ZrO_2, at 186 and 231 K with $\tau = 20$, 40, and 80 μs. The number adjacent to each line shape is the corresponding echo intensity normalized to the $\tau = 20$ μs intensity.

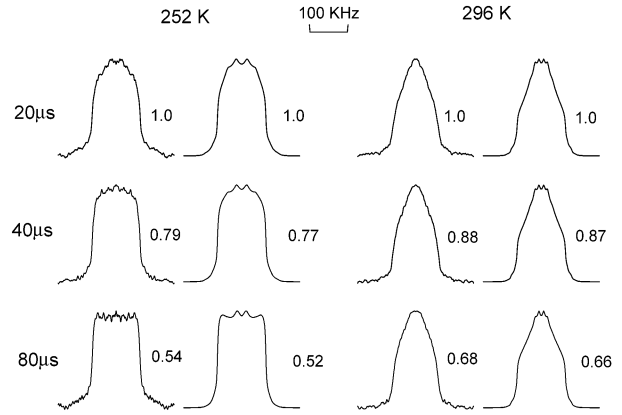

Figure 4. Experimental (left) and simulated (right) ^{2}H NMR spectra of HDCA-2,2-d_2 on ZrO_2, at 252 and 296 K with $\tau = 20$, 40, and 80 μs. The number adjacent to each line shape is the corresponding echo intensity normalized to the $\tau = 20$ μs intensity.

In Figures 3 and 4, the ^{2}H spectra of HDCA-d_2 monolayers, at several selected temperatures (186, 231, 252, and 296 K), are shown as a function of pulse delay time τ in the quadrupolar echo sequence. The number adjacent to each line shape is the echo intensity (i.e., signal intensity) normalized to the intensity of $\tau = 20$ μs. These spectra demonstrate that there are considerable variations in both the line shape and signal intensity with delay time τ. These variations testify to the presence of motions having correlation times in the range of $10^{-3}-10^{-6}$ s, that occur during the formation of the quadrupolar echo.[24]

Figure 5 shows the proton-decoupled ^{13}C spectrum of ^{13}C-labeled HDCA monolayers, $CH_3(CH_2)_{14}{}^{13}CO_2/ZrO_2$, obtained using a spectrometer operating at a higher field with a carbon resonance frequency of 125 MHz. The observed symmetric powder pattern suggests an axially symmetric chemical shift tensor for the carboxyl carbon. Shift tensors of carboxyl carbon in a number of simple acids, salts, and esters have been determined in the solid state.[25,26] The data show that, for compounds with "unidentate" carboxyl coordination such as acids and esters, the three principal values of the carboxyl tensor are quite different. As for solid metal acetates, principal values of 21 carboxyl tensors belonging to 14 different compounds are listed in ref 26. The average values and the standard deviations of the three principal elements of the 21 tensors are $\sigma_{11} = 231 \pm 5$, $\sigma_{22} = 205 \pm 8$, and $\sigma_{33} = 105 \pm 6$ ppm, giving an average asymmetry (η) of 0.35.[27] Unfortunately, the type of acetate ion coordination is known only for some of the compounds listed. Two of the compounds, cadmium acetate and zinc acetate, which have been demonstrated to contain acetate ions with bidentate chelating coordination,[28] show the lowest η values, 0.18 and 0.08, respectively. Although the size of the metal acetate database is relatively small, the data seem to imply a low η value ($\eta < 0.2$) for the bidentate chelating coordination. Simulation of the observed ^{13}C powder pattern, Figure 5, was also attempted and yielded an upper limit of 0.14 for the asymmetry parameter η. Thus, we considered the observation of a symmetric powder pattern ($\eta \approx 0$) as consistent with our earlier assertion of a bidentate chelating configuration for the alkanoic acid/ZrO_2 system.[12]

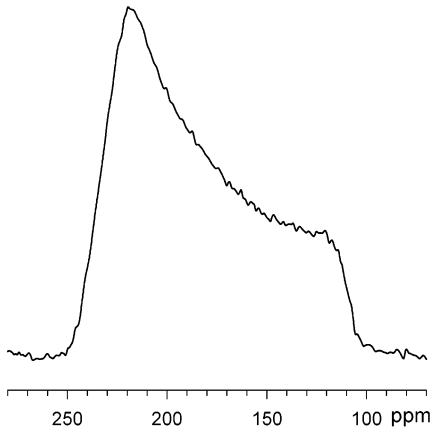

Figure 5. Proton-decoupled ^{13}C spectrum of ^{13}C-labeled HDCA monolayer, $CH_3(CH_2)_{14}{}^{13}CO_2$ on ZrO_2 powder, at room temperature taken with a spectrometer operating at a carbon resonance frequency of 125 MHz.

Discussion

First, we will consider simulation of the observed HDCA-d_2 spectra. Two types of motional processes, trans-gauche isomerization and axial diffusion, have been advanced for the interpretation of spectroscopic data concerning the dynamics of alkyl chains in several anisotropic and polymeric systems.[17,29,30] We do not consider axial diffusion around the chain axis as a possible motional mode for the adsorbed hexadecanoate. The two-dimensional ^{13}C NMR data of a closely related system (octadecanoate adsorbed on ZrO_2 powder) indicate that, at room temperature, the headgroup remains static on the deuterium NMR time scale.[12] Furthermore, this type of motions calls for a high uniform mobility at different methylene positions along the alkyl chain.[29b,31] This is in conflict with the significant increase of mobilities toward the untethered chain end as concluded from the spectra of the fully deuterated sample.

In consideration of two- or three-site jumps as possible simulation models, we note that for two site jumps the two C−D bond vectors describing the orientations prior and after the jump lie in a plane (actually they define the plane). In this sense, the two-site motions are considered as *planar* motions,[32,33] whereas jumps among three tetrahedral sites are not. As a consequence, for an aliphatic C−D bond undergoing two-site motions, one of the transverse principal components of the field gradient tensor (FGT) is not affected.[33] This constant principal component of FGT would in turn lead to powder spectra with a constant breadth of ~120 kHz. The fact that the experimental spectra of HDCA-d_2 do show a more or less constant breadth of this magnitude over the temperature range of 200 K to room temperature suggests the use of two-site jumps for simulation. Furthermore, several jump angles around the tetrahedral value of 109° were tested with the two-site jump model. It was found

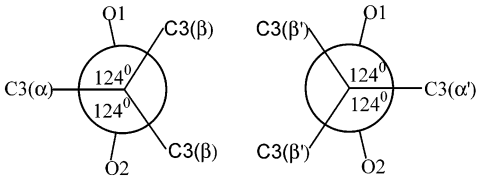

Figure 6. Newman projections along the C2−C1 bond, showing the orientations of the C2−C3 bond in the two sets of low energy conformers. Note that the conformer α (α′) is more stable than the conformer β (β').

that a jump angle of 113° yielded significantly better fits with the experimental line shapes, particularly in the middle part of the spectra.

To gain physical insight into this two-site model, a commercial molecular modeling program (Hyperchem from Hypercube Inc.) was employed to locate rotational isomers around the C1−C2 bond in isolated alkanoates. In accordance with a bidentate bond, the two oxygen atoms of the carboxylate group are assumed to be equivalent. The geometry of isolated molecules was first optimized using molecular mechanics with the standard MM+ force field parameters provided by the modeling program. In this optimized geometry, the three bond angles, O1−C1−O2, O1−C1−C2, and O2−C1−C2, were found to be 117.5°, 118.8°, and 118.8°, respectively. Therefore, the four atoms, C1, C2, O1, and O2, are not exactly on a plane; instead they adopt a slightly puckered configuration. A conformation search was then performed and yielded six low energy conformers around the C1−C2 bond, two more stable conformers (the α conformers) and four less stable conformers (the β conformers). Close examination reveals that the six conformers form two distinguishable groups or sets, which can be considered as mirror images of each other. Newman projections showing the orientations of the C2−C3 bond in these two sets are presented separately in Figure 6; note they are labeled as nonprimed (α and β) and primed (α′ and β') sets. Thus, the conformation search resulted in a six-site model with rotational jumping angles of ± (∼ 60°, ∼ 120°, and 180°) and, possibly, with three different jumping rates for α ↔ α, α ↔ β, and β ↔ β reorientation, respectively. Obviously, this six-site model bears no resemblance with the two-site jump model used in our simulation.

As clearly illustrated in Figure 6, the jumps between nonprimed and primed sets are accompanied by the flip−flop motions of the puckered configuration assumed by atoms C1, C2, O1, and O2. As mentioned in the first paragraph of the Discussion section, the two-dimensional ^{13}C NMR data of octadecanoate adsorbed on the same substrate indicate a static carboxylate group. Therefore, a second conformation search was performed assuming a rigid static headgroup, i.e., under the condition that no flip−flop of the puckered configuration is allowed. As expected, the search yielded only one of the two sets, i.e., three low energy conformers, one α and two β conformers. The two β conformers are related to the more stable α conformer by a rotational jump of 124° around the C1−C2 bond, the corresponding jump angle between C−D bond orientations is 113.9°. We speculate that molecules in the SAMs also adopt a puckered configuration that may even be strengthened or enhanced because of the bidentate chelating surface bonding, requiring two oxygen atoms to coordinate with one zirconium site. A jump angle of 113° can be rationalized if the atoms C1, C2, O1, and O2 of the adsorbed molecules adopt a rigid puckered configuration.

Even with a rigid puckered headgroup, the conformation search yielded three sites. However, we opted for a two-site model because the three site model with jumping angle of ∼113° will not result in spectra with a constant breadth of ∼120 kHz.[29a] Similarly, the two-site trans−gauche isomerization model has been applied to simulate ^{2}H spectra of deuterated alkyl chains observed in polymers,[34,35] lipid bilayers,[14,29] polymer model membranes,[30] and alkylsilyl-modified silica.[17] In all these cases, we are not dealing with an isolated gas-phase chain. It has been argued that conformation changes in a closed packed alkyl chain mostly probably proceed through cooperative motions such as kink 3-bond motions or crankshaft 5-bond motions. The crowded environment constrains the modes of isomerization and renders the two-site model appropriate for simulating conformational jumps at each segment of an alkyl chain.[29a,14,15]

In summary, the motional model assumed for spectral simulations is the two-site model with a jump angle set at 113°. The more populated lower energy site will be referred to as the α site and the other the β site. In all simulations, a quadrupole coupling constant of QCC = 168 kHz and an asymmetry parameter of $\eta = 0$ are assumed. The motions are characterized by jump rates $\Omega_{\alpha\rightarrow\beta}$ and $\Omega_{\beta\rightarrow\alpha}$, and site populations, P_α and P_β. In addition to $P_\alpha + P_\beta = 1$ these parameters must satisfy microscopic reversibility: $P_\alpha\Omega_{\alpha\rightarrow\beta} = P_\beta\Omega_{\beta\rightarrow\alpha}$, and therefore only two of the four parameters are independent. The product of the rate and its corresponding population such as $P_\alpha\Omega_{\alpha\rightarrow\beta}$ ($=P_\beta\Omega_{\beta\rightarrow\alpha}$) has been used as a quantitative measure of *molecular mobility*.[30] Comparison of molecular mobilities for motions described by the same model can thus be made by quoting their (PΩ) values.[19]

At all of the temperatures studied, it was found that reasonable fits with the experimental spectra could only be achieved by a weighted superposition of three or four line shapes computed assuming different rates and site populations. Examples of simulated line shapes and their relative intensities (the number adjacent to the corresponding line shape) are presented in Figures 3 and 4 with the corresponding experimental spectra. In computing relative intensities, we have also included the intensity decay arising from ^{1}H−^{2}H dipolar couplings. It is assumed that the latter has caused an additional intensity decay that is an exponential function of pulse delay τ with a time constant of 300 μs.[19,36−38] The parameters used for simulating the spectra, including those shown in Figures 3 and 4, are summarized in Table 1. Also included are the corresponding PΩ values, i.e., the values for molecular mobility. The estimated relative errors for these parameters depend on their magnitude; roughly speaking, they are ±15% for the populations P_β and for the component weights and ±(0.30 decade) for the reported rates (i.e., $\log((\Omega_{\text{reported}} + \Delta\Omega)/\Omega_{\text{reported}}) = \pm 0.30$).

We will first consider the experimental and simulated spectra at 296 K, the highest temperature studied. These spectra are presented, respectively, in the third (experimental) and forth (simulated) column of Figure 4. Careful examination reveals that the three experimental spectra, recorded with different τ delays, exhibit a round triangular top, whereas the corresponding simulated line shapes show a slightly broader center with a clearly noticeable middle dip. Spectra with a triangular top have also been observed at higher temperatures for several anisotropic and tethered chain systems.[17,19,29b,30] It can be shown that neither the two-site model with jump angle 113° nor the three-site jumping around a tetrahedral axis is capable of generating the triangular top such as the one observed in the room temperature (298 K) spectra, and therefore, models with more orientation sites must be invoked. A six-site model has been proposed and employed with reasonable success for line shape simulations in tethered chain systems.[17,19,29,30] This six-site model consists

TABLE 1: Spectral Simulation Parameters for the HDCA/ZrO_2 System

temp (K)	rate $\Omega_{\alpha\rightarrow\beta}$ (s^{-1})	β-site population, P_β	component weight	mobility, $P\Omega$	temp, (K)	rate $\Omega_{\alpha\rightarrow\beta}$, ($s^{-1}$)	β-site population, P_β	component weight	mobility, $P\Omega$
186	8.0×10^3	0.113	0.75	8.95×10^2	252	2.0×10^5	0.175	0.39	3.48×10^4
	1.3×10^5	0.013	0.12	1.59×10^3		1.6×10^5	0.263	0.19	4.18×10^4
	1.1×10^5	0.088	0.13	9.75×10^3		3.2×10^5	0.338	0.42	1.07×10^5
204	1.3×10^4	0.125	0.84	1.59×10^3	276	5.6×10^5	0.175	0.28	9.75×10^4
	8.0×10^4	0.038	0.08	2.98×10^3		7.2×10^5	0.275	0.24	1.97×10^5
	1.4×10^5	0.100	0.08	1.43×10^4		1.3×10^6	0.338	0.20	4.30×10^5
						1.6×10^6	0.438	0.28	6.97×10^5
231	1.4×10^4	0.175	0.60	2.51×10^3	296	5.6×10^5	0.225	0.20	1.25×10^5
	1.6×10^5	0.113	0.16	1.79×10^4		1.3×10^6	0.325	0.50	4.14×10^5
	9.6×10^4	0.225	0.24	2.15×10^4		3.2×10^6	0.438	0.14	1.39×10^6
						1.6×10^7	0.500	0.16	7.96×10^6

of three "trans" and three "gauche" sites, symmetrically placed around an all-trans chain axis. The model characterizes the site orientations and, hence, the terms "trans" and "gauche", in reference to the all-trans *alkyl* chain axis (C2 to C16 in our system) rather than to individual segments. The motions are similarly characterized by two independent parameters, the jump rate $\Omega_{t\rightarrow g}$ and the site population P_g. With the help of this model, we proceeded to simulate the room temperature spectra. Indeed the inclusion of small contributions (less than 15%) from this model enables us to eliminate the central dips and to achieve better fits with the room temperature spectra. It should be pointed out that, in our case, the model has only been used for simulating component line shapes for one temperature and that the total contribution of these component line shapes is relatively small. Therefore, we do not regard the better fits mentioned above as providing sufficient assurance that this particular model (or any other multisite model) is appropriate for our system. Additional data, for example, spectra at several elevated temperatures and the corresponding simulation results, will be required for making a reasonable judgment. For this reason, detailed descriptions of the six-site model and of the simulation results will not be given here.[39] However, we do expect that, above room temperature, an additional multisite (four or more sites) model will be needed for achieving reasonable fits with the ^2H spectra. With increasing temperatures, not only the motions occur with higher rates, additional sites also become available for the reorientation motion involving the C2−D bonds.

Two important conclusions can be drawn directly from the simulation results reported in Table 1. They are (a) the C2−D bonds show significant orientational freedom at all of the temperatures studied and (b) there is considerable motional heterogeneity in the HDCA monolayers as evidenced by the number of different line shapes required for simulation of the experimental spectra. Similar but somewhat higher mobilities have also been reported for the C1−D bonds of ODPA-d_2 molecules adsorbed on the same substrate.[19] On the other hand, the C1−D bonds of 1,1-d_2-octadecanethiol adsorbed on gold nanoparticles ($C_{18}S$/Au) remain essentially static at or below room temperature, as indicated by its ^2H NMR spectra.[22] It is well-known that the headgroup, the substrate, and the nature of surface bonding essentially dictate the structure of the monolayer.[2,9] Our results suggest that, by imposing structural constraints on the packing of the tethered chains, these factors exert a profound effect on the motional freedom of chain segments.

Previous studies have shown that the interchain spacing in tethered alkyl chain systems is determined by factors such as headgroup−substrate interactions, the size of the headgroup, and the orientation of the chain axis with respect to substrate surface. In the $C_{18}S$/Au system, the strong gold−sulfur bond plays a dominant role, leading to a $[(\sqrt{3} \times \sqrt{3})R30°]$ overlayer lattice and an area per chain of 21.7 Å^2.[2,9b] In addition, the chains cant from the surface normal by ∼30° reducing the effective interchain spacing and thus enhancing their van der Waals interactions. In the case of ODPA monolayers on powder ZrO_2, the estimated area per molecule of 24 Å^2 is mainly dictated by the large size of the phosphonate headgroup, and because of its unidentate bonding mode, the all-trans chains of the ODPA molecules are expected to adopt a nearly perpendicular orientation with respect to the substrate surface.[7a] For alkanoic acid monolayers, area densities from 21 to 30 Å^2/molecule have been measured on various substrates. For example, values of ∼ 21 Å^2/molecule have been reported for Lagmuir-Blodgett films on various aqueous mediums,[40] where the spacing is generally believed to be determined by interchain repulsions. On the other hand, for docosanoic acid monolayers on AgO an area per molecule of 28.8 Å^2 and a chain tilt of (26 ± 1°) with respect to the surface normal have been obtained from surface X-ray diffraction data.[41] These and other data on similar systems also indicate that the carboxylate moiety is bound symmetrically, strongly suggesting a bidentate binding mode involving two equivalent carboxylate oxygen atoms.[11] Furthermore, in the symmetric carboxyl configuration, the C1−C2 bond adopts an orientation nearly perpendicular to the substrate surface. As a consequence, an all-trans alkyl chain is expected to lie at a tilt angle of ∼30° with respect to the surface normal, which is very close to the experimental value of 26° found for docosanoic acid monolayers on AgO. As concluded from our earlier study, the alkanoate molecules bind zirconia surface via a bidentate chelating bond through two equivalent carboxylate oxygen atoms.[12] In view of the similarity in their binding configurations, we argue that an area of 26−30 Å^2/molecule can be reasonably assumed for HDCA molecules in our system. As mentioned above, tilting chain configurations in octadecanethiolate, docosanoic acid, and presumably HDCA SAMs enhance the van der Waals interactions and thus impose additional constraints on reorientation motions. Therefore, the high mobility observed for HDCA monolayers can be attributed at least partially to the surface binding configuration resulting in a large interchain spacing, whereas in the case of ODPA monolayers, it can be attributed to both the size of the headgroup and the nearly perpendicular orientation adopted by the alkyl chain.

In accordance with our motional models, the reorientation process involves rotational jumps around the C1−C2 bond with respect to the two C−O bonds in the headgroup. Rotational barriers in a number of simple gas phase compounds have been measured with microwave spectroscopy. The available data suggest that methyl groups attached to a carbonyl carbon atom show significantly lower potential barriers to internal rotation in comparison with ethane.[42] For example, potential barriers for methyl rotation in ethane, acetone, and acetic acid are 12.3, 3.26,

and 2.02 kJ/mol, respectively. In comparison, the measured potential barrier to methyl rotation in methanethiol is 5.31 kJ/mol. Unfortunately, similar data are not available for phosphonate compounds. If the trend mentioned above also holds for the $-CD_2R$ group rotation, a lower rotation barrier could be expected for rotations around the C1−C2 bond in HDCA. This could facilitate cooperative motions involving the C1−C2 bond such as coupled gauche rotations leading to the formation of kinks or jogs.

The surface of ZrO_2 is known to be complex containing different types of surface sites.[43] As discussed in ref 12, the broadness of both the C−O stretching bands in IR and the carboxylate resonance in ^{13}C CP-MAS NMR are indications of a heterogeneous bonding environment experienced by the adsorbed HDCA molecules on the zirconia powder surface. Likewise the motional heterogeneity as revealed by our simulation results can be considered as a reflection of the complex nature of the ZrO_2 surface. Furthermore the component weights reported in Table 1 show considerable variations with temperature suggesting the absence of well-defined domains with respect to the orientational freedom of the alkyl chain. We interpret the varying weights as an indication that there are two or more factors affecting the reorientational freedom. In addition to surface properties of ZrO_2, other factors such as the local chain packing density, chain tilt angles, and surface defects can also affect motional freedom. Similar bonding and motional heterogeneity are observed for ODPA monolayers on the same substrate as evidenced by the ^{31}P NMR and ^2H NMR data.[7,19] However, careful examination of the deuterium simulation results of HDCA monolayers with those of ODPA monolayers indicates there are subtle differences concerning the bond reorientation motions in these two systems. The range of kinetic parameters covered by component line shapes for individual spectral simulation can be visualized by plotting the rates and site populations of the line shapes as abscissas and ordinates, respectively. Figure 7 shows such plots for these two systems at several comparable temperatures; line shapes from two-site and six-site models are marked with symbols □ and ○, respectively. For HDCA, either the components have similar kinetic parameters (at low temperatures) or the dispersion mainly occurs in one "dimension", i.e., in the site populations (at higher temperatures). On the other hand, the plots for ODPA show dispersions in both the rates and the site populations at all temperatures studied. Thus, a higher degree of motional heterogeneity exists within the ODPA monolayers. The varying characters of the surface sites seem to have a lesser effect on the binding of carboxylic groups as compared to that of phosphonate groups. In this respect, we notice that the alkanoic acids bind to the surface via a bidentate chelating bond, which requires the cooperation of the two carboxylate oxygen atoms in their interaction with the substrate surface.

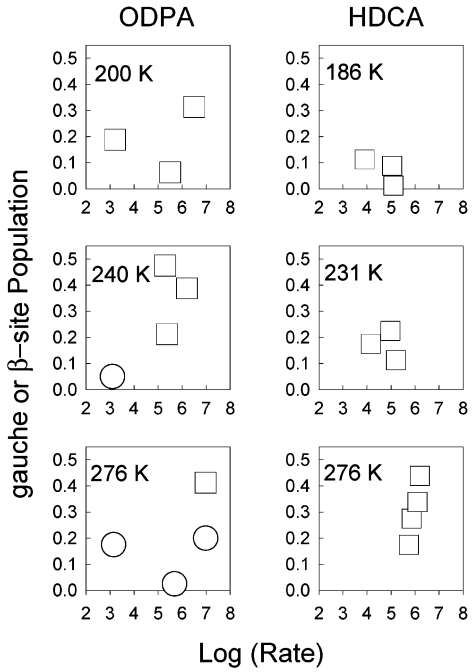

Figure 7. Kinetic parameters, site populations as ordinates and log(rates) as abscissas, of the component line shapes at three different temperatures for ODPA/ZrO_2 (left) and HDCA/ZrO_2 (right) systems. Note that line shapes from two-site and six-site models are marked with symbols □ and ○, respectively, and the size of the symbol roughly indicates the estimated error range.

Conclusions

The observed ^2H NMR spectra and their temperature dependence reveal the presence, in the HDCA monolayers, of a considerable motional gradient along the alkyl chain. For simulating ^2H spectra of adsorbed HDCA-d_2 molecules, we outlined a motional model that can account for the important spectral features and trends. We further argued that the proposed model is consistent with the above-mentioned motional gradient and other known spectroscopic evidences and also with the bidentate surface bonding mode involving the carboxylic headgroup. However, this does not offer assurance that some other models will not fit the experimental data equally well or better. We are of the opinion that our model has furnished a consistent, although somewhat simplified, picture which allows more quantitative discussion concerning the dynamics and the environment of the hexadecanoate molecules in the monolayers.

We have shown that, within the temperature range studied, the C2−D bonds of the attached HDCA molecules undergo reorientational motions with rates fast enough to affect the ^2H solid echo spectra. The fast reorientation rates can be attributed to the bidentate chelating bonding configuration leading to a large interchain spacing and to the low rotational barrier around the C1−C2 bond. Dynamic behaviors of several SAMs were compared to examine the effect of various factors on the reorientation dynamics of the C−C bond next to the headgroup. The results clearly illustrate the dominant role played by the headgroup and its interactions with the substrate surface.

We have established that there exists substantial motional heterogeneity in the HDCA monolayers. The heterogeneity observed in both the motional freedom and chain conformation reflects the complex nature of the ZrO_2 surface. Our simulation results further suggest that a higher degree of motional heterogeneity exists in the ODPA/ZrO_2 system as compared to the HDCA/ZrO_2 system.

Acknowledgment. Financial support from the Quebec Government (FQRNT) is gratefully acknowledged.

References and Notes

(1) (a) Allara, D. L.; Nuzzo, R. G. *Langmuir* **1985**, *1*, 45. (b) Allara, D. L.; Nuzzo, R. G. *Langmuir* **1985**, *1*, 52. (c) Schlotter, N. E.; Porter, M. D.; Bright, T. B.; Allara, D. L. *Chem. Phys. Lett.* **1986**, *132*, 93.

(2) Ulmann, A. *Chem. Rev.* **1996**, *96*, 1533.

(3) Ulmann, A. *An Introduction to Ultrathin Organic Films*; Academic Press: Boston, MA, 1991.

(4) (a) Cao, G.; Hong, H.-G.; Mallouk, T. E. *Acc. Chem. Res.* **1992**, *25* (5), 420. (b) Lee, H.; Kepley, L. J.; Hong, H.-G.; Mallouk, T. E. *J. Am. Chem. Soc.* **1988**, *110*, 618. (c) Lee, H.; Kepley, L. J.; Hong, H.-G.; Mallouk, T. E. *J. Phys. Chem.* **1988**, *92*, 2597.

(5) Katz, H. E. *Chem. Mater.* **1994**, *6*, 2227.

(6) Thompson, M. E. *Chem. Mater.* **1994**, *6*, 1168.

(7) (a) Gao, W.; Dickinson, L.; Grozinger, C.; Morin, F. G.; Reven, L. *Langmuir* **1996**, *12*, 6429. (b) Gao, W.; Dickinson, L.; Grozinger, C.; Morin, F. G.; Reven, L. *Langmuir* **1997**, *13*, 115.

(8) Folkers, J. P.; Gorman, C. B.; Laibinis, P. E.; Buchholz, S.; Whitesides, G. M.; Nuzzo, R. G. *Langmuir* **1995**, *11*, 813.

(9) Bishop, A. R.; Nuzzo, R. G. *Curr. Opin Colloid Interface Sci.* **1996**, *1*, 127. (b) Dubois, L. H.; Nuzzo, R. G. *Annu. Rev. Phys. Chem.* **1992**, *43*, 437.

(10) (a) Badia, A.; Lennox, R. B.; Reven, L. *Acc. Chem. Res.* **2000**, *33*, 475. (b) Reven, L.; Dickinson, L. *Thin Films* **1998**, *24*, 149.

(11) (a) Tao, Y. T. *J. Am. Chem. Soc.* **1993**, *115*, 4350. (b) Tao, Y. T.; Lee, M. T.; Chang, S. C. *J. Am. Chem. Soc.* **1993**, *115*, 9547.

(12) Pawsey, S.; Yach, K.; Halla, J.; Reven, L. *Langmuir* **2000**, *16*, 3294.

(13) (a) Risse, T.; Hill, T.; Schmidt, J.; Abend, G.; Hamann, H.; Freund, H.-J. *J. Phys. Chem. B* **1998**, *102*, 2668. (b) Risse, T.; Hill, T.; Schmidt, J.; Abend, G.; Hamann, H.; Freund, H. J. *J. Chem. Phys.* **1998**, *108*, 8615.

(14) Griffin, R. G. *Methods Enzymol*. **1981**, *72*, 108.

(15) Spiess, H. W. *Adv Polym. Sci*. **1985**, *66*, 24.

(16) Vold, R. R.; Vold, R. L. *Adv. Magn. Opt. Reson.* **1991**, *16*, 85.

(17) Zeigler, R. C.; Maciel, G. E. *J. Am. Chem. Soc*. **1991,** *113*, 6349.

(18) Kang, H.-J.; Blum, F. D. *J. Phys. Chem.* **1991**, *95*, 9391.

(19) Yim, C. T.; Pawsey, S.; Morin, F. G.; Reven, L. *J. Phys. Chem. B* **2002**, *106*, 1728.

(20) Wittebort, R. J.; Olejniczak, E. T.; Griffin, R. G. *J. Chem. Phys*. **1987**, *86*, 5411.

(21) Yim, C. T.; Gilson, D. F. R.; Budgell, D. R.; Gray, D. G. *Liq. Cryst.* **1993**, *14*, 1445.

(22) Badia, A.; Cuccia, L.; Demers, L.; Morin, F.; Lennox, R. B. *J. Am. Chem. Soc*. **1997**, *119*, 2682.

(23) Zeigler, R. C.; Maciel, G. E. *J. Phys. Chem.* **1991**, *95*, 7345.

(24) Spiess, H. W.; Sillescu, H. *J. Magn. Reson.* **1981**, *42*, 381.

(25) Veeman, W. S. *Prog. NMR Spectrosc.* **1984**, *16*, 193.

(26) Duncan, T. M. *A Compilation of Chemical Shift Anisotropies*, 2nd ed.; Farragut Press: Chicago, IL, 1997.

(27) Here the asymmetry η is given by $\eta = ((\sigma_{11}-\sigma_{22})/(\sigma_{iso}-\sigma_{33}))$ where $\sigma_{iso} = (\sigma_{11} + \sigma_{22} + \sigma_{33})/3$.

(28) Deacon, G. B.; Phillips, R. J. *Coord. Chem. Rev.* **1980**, *33*, 227.

(29) (a) Huang, T. H.; Skarjune, R. P.; Wittebort, R. J.; Griffin, R. J.; Oldfield, E. *J. Am. Chem. Soc.* **1980**, *102*, 7377. (b) Blume, A.; Rice, D. M.; Wittebort, R. J.; Griffin, R. G. *Biochemistry* **1982**, *21*, 6220.

(30) (a) Ebelhauser, R.; Spiess, H. W. *Makromol. Chem*. **1987**, *188*, 2935. (b) Ebelhauser, R.; Spiess, H. W. *Ber. Bunsen-Ges. Phys. Chem.* **1985**, *89*, 1208.

(31) Clauss, J.; Schmidt-Rohr, K.; Adam, A.; Boeffel, C.; Spiess, H. W. *Macromolecules* **1992**, *25*, 5208.

(32) The term "jump" is employed by simulation programs to imply that the reorientation process occurs instantaneously and involves no intermediate states. At any given instant each bond must have one of the orientations of the possible sites. Spectral simulations provide no information concerning the nature of the jumping process, and therefore they are incapable of distinguishing, for example, rotational jumps from nonrotational jumps (e.g., puckering motions).

(33) Hirschinger, J.; English, A. D. *J. Magn. Reson.* **1989**, *85*, 542.

(34) Hentschel, H.; Sillescu, H.; Spiess, H. W. *Polymer* **1984**, *25*, 1078.

(35) Jelinski, L. W.; Dumais, J. J.; Engel, A. K. *Marcomolecules* **1983**, *16*, 492.

(36) Yim, C. T.; Brown, G. R.; Morin, F. *Langmuir* **1997**, *13*, 4383.

(37) (a) Hirschinger, J.; Miura, H.; Gardner, K. H.; English, A. D. *Macromolecules* **1990**, *23*, 2153. (b) Miura, H.; Hirschinger, J.; English, A. D. *Macromolecules* **1990**, *23*, 2169.

(38) Kintanar, A.; Huang, W. C.; Schindele, D. C.; Wemmer, D. E. Dorbny, G. *Biochemistry* **1989**, *28*, 282.

(39) A detailed description of the six-site model can be found in our previous publication (ref 19), which deals with the octadecylphosphonate (ODPA) monolayers on the same substrate. The simulation parameters for the best fits are (number of sites, rate $\Omega_{\alpha\rightarrow\beta}$ or $\Omega_{t\rightarrow g}$, population P_β or P_g, weight): (2, 7.2×10^5, 0.188, 0.40); (2, 9.6×10^5, 0.275, 0.24); (2, 3.2×10^6, 0.275, 0.24); (6, 9.6×10^5, 0.300, 0.08); (6, 9.6×10^6, 0.300, 0.04).

(40) Hann, R. A. In *Langmuir*−*Blodgett Films*; Robert, G., Ed.; Plenum Press: New York, 1990; Chapter 2,

(41) Samant, M. G.; Brown, C. A.; Gordon, J. G. *Langmuir* **1993**, *9*, 1082.

(42) (a) Lister, D. G.; MacDonald, J. N.; Owen, N. L. *Internal Rotation and Inversion*; Academic Press: London, 1978. (b) Durig, J. R.; Craven, S. M.; Harris, W. C. In *Vibrational Spectra and Structure*; Durig, J. R., Ed.; Dekker: New York, 1972; Vol. 1, p 73.

(43) (a) Schafer, W. A.; Carr, P. W.; Funkenbusch, E. F.; Parson, K. A. *J. Chromatogr.* **1991**, *587*, 137. (b) Nawrocki, J.; Dunlap, C. J.; Carr, P. W.; Blackwell J. A. *Biotechnol. Prog.* **1994**, *10*, 561.